ARTICLE

Insights from genetic and demographic connectivity for the management of rays and skates

Florianne Marandel, Pascal Lorance, Marco Andrello, Grégory Charrier, Sabrina Le Cam, Sigrid Lehuta, and Verena M. Trenkel

Abstract: Studying demographic and genetic connectivity can help assess marine metapopulation structure. Rays and skates have no larval phase; hence, population connectivity can only result from active movement of individuals. Using thornback ray (*Raja clavata*) in European waters as a case study, demographic and genetic connectivity were studied for 11 putative populations with unequal population abundances and two hypotheses of dispersal rates. Genetic simulation results highlighted three large metapopulations: in the Mediterranean, around the Azores, and on the Northeast Atlantic shelf. Demographic results highlighted a finer population structure indicating that several pairs of putative populations might be demographically linked. Results were highly sensitive to dispersal assumptions and relative population abundances, which provided insights into the potential magnitude of genetic and demographic connectivity differences. Accounting for demographic connectivity appears to be crucial for managing and conserving rays and skates, while genetic connectivity provides a longer-term perspective and less subtle spatial structures. Moreover, accounting for heterogeneity in population abundances is a key factor for determining or interpreting metapopulation connectivity.

Résumé : L'étude de la connectivité démographique et génétique peut aider à évaluer la structure des métapopulations marines. Les raies n'ont pas de stade larvaire, de sorte que la connectivité des populations ne peut découler que de déplacements actifs d'individus. Utilisant le cas de la raie bouclée (*Raja clavata*) dans les eaux européennes, nous avons étudié la connectivité démographique et génétique pour 11 populations présumées en simulant des abondances inégales des populations ainsi que deux hypothèses de dispersion. Les résultats des simulations génétiques font ressortir trois grandes métapopulations, une dans la Méditerranée, une autour des Açores et une sur le plateau continental de l'Atlantique nord-est. Les résultats démographiques font ressortir une structure de populations plus fine qui indique que plusieurs paires de populations présumées pourraient être reliées du point de vue démographique. Les résultats sont très sensibles aux hypothèses concernant la dispersion et aux abondances relatives des populations, ce qui fournit de l'information sur l'ampleur possible des différences de connectivité génétique et démographique. La prise en considération de la connectivité démographique semble revêtir une importance clé pour la gestion et la conservation des raies, alors que la connectivité génétique fournit une perspective à plus long terme et des structures spatiales moins fines. La prise en considération de l'hétérogénéité de l'abondance des populations constitue en outre un facteur clé pour déterminer ou interpréter la connectivité de métapopulations. [Traduit par la Rédaction]

Introduction

Population connectivity is a crucial parameter to take into account when defining population units relevant for management and conservation purposes (Stearns and Hoekstra 2005; Sinclair et al. 2006; Schwartz et al. 2007). Population units relevant for management purposes are commonly defined using ecological and genetic information. For example, the degree of connectivity between populations can be assessed by the amount of exchanged individuals (Waples and Gaggiotti 2006). By reproducing in the population they joined, these individuals contribute to the local demography but also transfer their genetic material into the gene pool, thus inducing gene flow among populations. A metapopulation is a network of local populations that exchanges individuals but has somewhat independent dynamics (Levins 1969). Determining how many local or metapopulations exist and characterizing the relationships among them is a challenging task. Numerous definitions of the population concept exist (see Waples and Gaggiotti 2006). Almost all involve interbreeding individuals over a geographical area. However, they lack objective and quantitative criteria for delimiting distinct populations. In this context, different researchers might identify different population structures based on the same information (Waples and Gaggiotti 2006).

F. Marandel, P. Lorance, S. Lehuta, and V.M. Trenkel.* Institut Français de Recherche pour l'Exploitation de la Mer (Ifremer), BP 21105, 44311 Nantes cedex 3, France.
M. Andrello. EPHE, PSL Research University, CEFE UMR 5175, CNRS, Université de Montpellier, Biogéographie et Ecologie des Vertébrés, 1919 route de Mende, 34293 Montpellier, France.
G. Charrier. Université de Bretagne Occidentale, Laboratoire des Sciences de l'Environnement Marin (LEMAR, UMR 6539 CNRS/IRD/UBO/Ifremer), Technopôle Brest-Iroise, 29280 Plouzané, France.
S. Le Cam. Université de Bretagne Occidentale, Laboratoire des Sciences de l'Environnement Marin (LEMAR, UMR 6539 CNRS/IRD/UBO/Ifremer), Technopôle Brest-Iroise, 29280 Plouzané, France; Institut Français de Recherche pour l'Exploitation de la Mer (Ifremer), Avenue de Mus de Loup, Ronce les Bains, 17390 La Tremblade, France.

Corresponding author: Florianne Marandel (email: florianne.marandel@ifremer.fr).
*Verena M. Trenkel currently serves as an Associate Editor; peer review and editorial decisions regarding this manuscript were handled by Eric Taylor.

1292

Can. J. Fish. Aquat. Sci. Vol. 75, 2018

Population connectivity has two components: genetic and demographic. Genetic connectivity is defined as the degree to which gene flow affects evolutionary processes within populations, and demographic connectivity is the relative contribution of dispersal to population dynamics (Lowe and Allendorf 2010). The two components inform on population connectivity at evolutionary and ecological time scales, respectively. For example, high genetic connectivity does not necessarily imply high demographic connectivity and that a single unit should be considered for management (Hawkins et al. 2016).

On one hand, genetic connectivity is often derived from the measure of genetic differentiation between populations shaped by the interplay of the four evolutionary forces (gene flow, genetic drift, selection, and mutation; Hallerman 2003; Stearns and Hoekstra 2005). Their respective magnitude is greatly dependant on population abundance, and only gene flow is relevant as the genetic component of population connectivity. Therefore, depending on the population abundance, genetic differentiation can be a poor proxy of gene flow. For example, in the case of large populations, genetic differentiation can remain weak despite reduced levels of gene flow because of a very low genetic drift. In studies of genetic population structure, the absolute number of migrants is used preferentially to the migration rate, as it conveys information on population abundance, i.e., census population size (Palumbi 2003). However, knowledge on population abundance is often lacking, especially for marine populations.

On the other hand, demographic population structure greatly depends on life history traits. Indeed, following the definition above of demographic connectivity, demographically connected populations display intrinsic growth or survival rates that are reciprocally affected by immigration or emigration (Lowe and Allendorf 2010). Thus, evaluation of demographic connectivity requires information on the contribution of dispersal but also on the demographic rates and abundance of each population. This information is not only needed for assessing the effect of dispersal on population growth rates but also for defining threshold values for demographic connectivity. Despite the importance of demographic connectivity for defining management units, defining appropriate thresholds for demographically connected populations has received relatively little attention in the literature (Waples and Gaggiotti 2006; Waples et al. 2008). Importantly, for both genetic and demographic connectivity studies, dispersal is a central process that we define as an individual leaving the home range of its birth population to move to another population's home range, the movement being one way and not a round trip (Dingle 2014).

In this study, we evaluated the use of genetic and demographic connectivity for identifying management units of rays and skates. Bycaught in several fisheries, many populations of skates and rays have declined, sometimes strongly, in the Northeast Atlantic during the 20th century (Quéro and Cendrero 1996; Dulvy et al. 2014). Therefore, the conservation of these species has become a major objective for ensuring sustainable exploitation of marine resources (Dulvy et al 2014; Davidson et al. 2016). For reaching this objective, it is fundamental to delimit appropriate management units. However, for many species, available data are restricted to life history traits (though not always available for all populations), landings, and, only in some cases, survey time series informing on abundance changes (ICES 2016). In European waters, recent landings levels of most ray and skate species differ greatly among the southern North Sea, the western Mediterranean Sea, and the Azores, which can be considered indicative of differences in population abundances, as there are no species-specific catch quotas in place for these species (Fig. 1a) (ICES 2016).

In contrast with teleosts, rays and skates have a low potential for dispersal and thus gene flow. They produce few offspring that develop in egg capsules fixed to the seabed during several months (Hoening and Gruber 1990). As there is no pelagic larval stage that can be dispersed by marine currents, the dispersal of rays and skates is solely based on the movements of juveniles and (or) adults. Ovenden (2013) argued that due to dispersal happening at later life stages, elasmobranch species might present crinkled connectivity, which she defined as a situation where dispersal is large enough to make populations genetically similar but too small to matter for demographic connectivity.

For several medium-sized ray species, comparable degrees of movement between adjacent populations have been observed (Walker et al. 1997; Hunter et al. 2005a, 2005b; Stephan et al. 2015). However, for two ray species sharing similar life history traits and overlapping spatial ranges, genetics studies have indicated distinct structuring patterns. The thornback ray (*Raja clavata*) seems to display strong spatial genetic differentiation (Chevolot et al. 2006), while the thorny skate (*Amblyraja radiata*) presents only weak although statistically significant differentiation (Chevolot et al. 2007). These contrasting results could be due to differences in dispersal behavior, despite similar biology, along the continental shelf edge, which might not constitute a barrier for thorny skate but it could be one for thornback ray (Chevolot 2006). However, while dispersal is a necessary condition for connectivity, it is not sufficient because dispersed individuals need to reproduce in the receiving population. So the difference could also be caused by differential integration into the spawning components.

In this study, we evaluated the use of genetic and demographic connectivity for identifying management units of rays and skates. We use the term "putative population" for assumed populations occurring at discrete sampling locations. Demographic and genetic criteria are applied to these putative populations to evaluate their connectivity. We used a modelling approach with life history parameters resembling those of thornback ray, a typical widespread ray species in European waters. This species is the most studied ray in the Northeast Atlantic. Its biological parameters are representative for medium-bodied skates and rays (refer to online Supplementary Table S1[1]). Similar to other rays and skates, local abundances of thornback ray differ strongly, taking recent landings as an indication of population abundances (Fig. 1a). As no reliable dispersal rate estimates were available on a European scale (but see Walker et al. 1997 for regional dispersal values), we defined plausible scenarios based on expert knowledge. Genetic connectivity was evaluated by calculating the fixation index F_{ST} defined by Wright (1949). In contrast, we did not evaluate demographic connectivity sensus stricto, as the effect of dispersal on population growth rates was not investigated directly. Instead, we evaluated whether the number of dispersed individuals was likely to contribute to local population abundances. In addition, using a matrix model we identified the life history parameters and life stages to which the population growth rate was most sensitive. These results provided context for interpreting the importance of dispersal for population growth.

Materials and methods

Life history parameters and intrinsic population growth

Usher matrix model

To appraise the potential importance of dispersal for population dynamics of a thornback ray-like species, we studied the sensitivity and elasticity of intrinsic population growth rate to variations and uncertainty in life history traits. To this aim we used an Usher matrix model (Usher 1966). The model consisted of four life stages grouping ages with similar demographic parameters:

Fig. 1. (*a*) Standardized mean landings 2013–2015 ((value – min.)/(max. – min.)) of ten skate and ray species from the Northeast Atlantic grouped by spatial distribution pattern (spatial units as in panel (*b*)). Spatial units considered as single stocks by the International Council for Exploration of the Sea are connected by solid lines. (*b*) Thornback ray putative populations with dispersal paths (black solid lines). 200 m isobaths are shown in grey. Figure created using R statistical software and the "PBSmapping" package (Schnute et al. 2017).
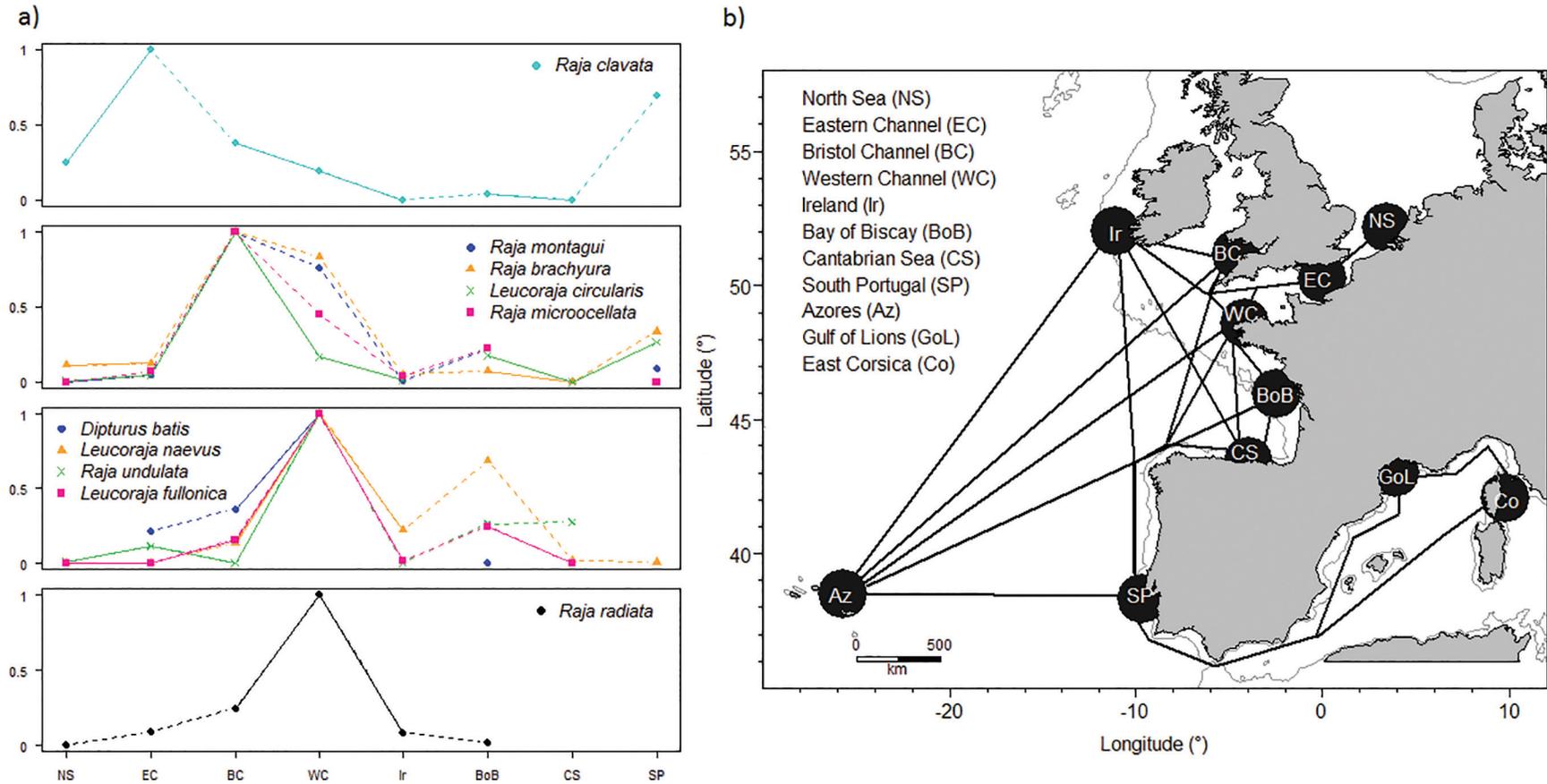
Table 1. Parameters values used in the Usher matrix model for the local elasticity as well as the minimum and maximum values used for the global sensitivity (Morris) analysis.

Parameter	Description	Baseline value	Alternative value	Morris method	
				Min.	Max.
Ω_4	No. of eggs stage 4	150[a]	48[b]	40	150
S_0	Egg and newborn survival	0.036[c]	0.01	0.01	0.5
S_1	Survival stage 1	0.20[c]	0.40	0.1	0.99
S_2	Survival stage 2	0.69[c]	0.40	0.1	0.99
S_3	Survival stage 3	0.81[c]	0.90	0.1	0.99
S_4	Survival stage 4	0.48[c]	0.90	0.1	0.99
H_2	Maturation rate stage 2	0.2[d]	0.3	0.05	1
H_3	Rate of fecundity increase stage 3	0.1[d]	0.2	0.05	1

[a]Holden et al. 1971.
[b]Ellis and Shackley 1995.
[c]Derived in this study.
[d]Educated guess.

stage 1 included age 1 individuals, stage 2 ages 2 to 6 (immature), stage 3 ages 7 to 11 (mature individuals), and stage 4 ages 12 years and older (highly fecund mature individuals).

$$(1) \qquad N_{t+1} = UN_t, \quad U = \begin{pmatrix} 0 & 0 & S_0 f_3 & S_0 f_4 \\ S_1 & S_2(1-H_2) & 0 & 0 \\ 0 & S_2 H_2 & S_3(1-H_3) & 0 \\ 0 & 0 & S_3 H_3 & S_4 \end{pmatrix}$$

where N_t is the vector of abundance by life stage, and U is the transition matrix. Each life stage s has a specific survival rate S_s. A maturation rate H_2 between stages 2 and 3 was derived from expert knowledge. S_0 is first year survival (from egg laying to 1 year). Fecundity was assumed to depend on the number of eggs Ω_s produced and the proportion of females $P_\female$ ($f_s = \Omega_s P_\female$). Stage 3 was assumed less fecund than stage 4; this was achieved by setting the number of eggs to $\Omega_3 = 0.7\Omega_4$. So H_3 represents an increase in the rate of fecundity between stages 3 and 4. A sex ratio of 1:1 was assumed ($P_\female = 0.5$), which is typical for rays and skates (Steven 1933; Ellis and Shackley 1995; Delpiani 2016).

Survival rate estimates were obtained in the following way. First, size-at-age L_a was estimated using the von Bertalanffy equation with growth parameters t_0, K, and L_∞ from the literature (Serra-Pereira et al. 2008). Second, mortality-at-age M_a was estimated using the empiric relationship developed by Gislason et al. (2010):

$$(2) \qquad \ln(M_a) = 0.55 - 1.61 \ln(L_a) + 1.44 \ln(L_\infty) + \ln(K)$$

Third, mortality M_a was transformed to survival-at-age $S_a = \exp(-M_a)$. To account for senescence, survival was reduced from age 12 onwards (Fig. S1 in electronic Supplementary material[1]). Survival by life stage was calculated by averaging over the corresponding ages (except for S_1). As no information was available for first year survival (S_0), the value was chosen to lead to a stable population. All baseline parameter values are summarized in Table 1.

Elasticity and sensitivity analyses

At equilibrium, the first positive eigenvalue of U (eq. 1) corresponds to the intrinsic population growth rate λ. Local elasticity and global sensitivity analyses were conducted to identify the life history parameters and life stages the value of λ was most sensitive to.

Elasticity represents the relative change in population growth rate in response to a certain relative change in vital rate parameters $P_i \in (\Omega_4, S_0, S_1, S_2, S_3, S_4, H_2, H_3)$. Thus, elasticity can be compared for parameters of different unit, such as survival rates S_s ($0 \le S_s \le 1$) and the number of eggs ($0 \le \Omega_4$).

Elasticity E of population growth rate λ to changes in parameter P was defined as follows (Caswell 2001):

$$(3) \qquad E = \frac{P_i}{\lambda} \frac{\Delta\lambda}{\Delta P_i}$$

Two types of parameter value changes were tested one parameter at a time: alternative parameter values based on available data or expert guess and a ±10% change of all baseline parameter values (Table 1).

The global sensitivity analysis was carried out using the Morris (1991) method improved by Campolongo et al. (2007) and Pujol (2009). The method consists of calculating successively the so-called elementary effect, which corresponds to the change in the intrinsic population growth rate λ when the current value of P_i is changed successively by adding or subtracting Δ_i along trajectories, holding all other parameter values constant, divided by Δ_i:

$$(4) \qquad d_i(P) = \frac{\lambda(P_{\Delta_i}) - \lambda(P)}{\Delta_i}$$

The step size Δ_i for each parameter was defined as

$$(5) \qquad \Delta_i = \frac{\max(P_i) - \min(P_i)}{k}$$

These elementary effects are computed at various locations of the parameter space so interaction effects can be evidenced. Here, $k = 0$ was used and rather extreme maximum and minimum parameter values were chosen (Table 1). The method uses an efficient sampling design that led to 16 200 estimates of $d_i(P)$. These were then summarized by calculating for each parameter P_i the mean of absolute effects $\mu_i^* = \overline{|d_i(P)|}$, which quantifies sensitivity, and the variance σ^2, which informs on the strength of interactions. All calculations were carried out in R using the package "sensitivity" setting the number of elementary effect computed per factor to 1800 (V1.14.0; Pujol et al. 2014). Calculations were repeated 10 times to ensure convergence.

Evaluating connectivity

Dispersal between putative populations

For evaluating demographic and genetic connectivity, 11 putative populations of thornback ray were assumed, based mainly on

Table 2. Mean landings of thornback ray for the period 2013–2015, simulated population sizes for the 11 studied locations, ICES stock identity for nine locations (Mediterranean stocks are not covered by ICES), and membership of putative populations to genetic and demographic units derived from modeling results (see text) for dispersal scenarios 1 (SC1) and 2 (SC2).

Code	Location (ICES division)	Landings (tonnes)	Simulated population size	ICES stock identity	Genetic units (Gu)		Demographic units (Du)	
					SC1	SC2	SC1	SC2
NS	North Sea (4c)	427.3[a]	125 000	rjc-347d	Gu1	Gu1	Du1	Du1
EC	Eastern Channel (7d)	1112.9[a]	300 000	rjc-347d	Gu1	Gu1	Du1	Du1
BC	Bristol Channel (7fg)	549.4[a]	165 000	rjc-7afg	Gu1	Gu1	Du1	Du1
WC	Western Channel and Southern Celtic Sea (7he)	378.9[a]	90 000	rjc-echw	Gu1	Gu1	Du1	Du1
Ir	Ireland (7bcjk)	204.0[a]	50 000	Grouped with other Rajidae	Gu1	Gu1	Du1	Du1
BoB	Bay of Biscay (8ab)	241.4[a]	60 000	rjc-bisc	Gu1	Gu1	Du1	Du2
CS	Cantabrian Sea (8c)	204.9[a]	60 000	rjc-bisc	Gu1	Gu1	Du1	Du3
SP	South Portugal (9a)	840.4[a]	215 000	rjc-pore	Gu1	Gu1	Du1	Du3
Az	Azores (10)	180.0[b]	50 000	Grouped with other Rajidae	Gu2	Gu2	Du2	Du4
GoL	Gulf of Lion	15.2[c]	10 000	NA[d]	Gu3	Gu3	Du3	Du5
Co	Corsica	NA	10 000	NA[d]	Gu4	Gu4	Du4	Du6

[a]ICES 2016.
[b]Unpublished data.
[c]FAO 2016.
[d]Not covered by ICES.

expert judgement and results from a population genetics study (Chevolot et al. 2006) (Fig. 1b). Only a few tagging studies were available for medium-sized skate and ray species, but all showed recapture or travelling distances less than 150 km (Supplementary Table S1[1]; Walker et al. 1997; Hunter et al. 2005a, 2005b). The International Council for the Exploration of the Sea (ICES) currently assesses several of these 11 putative populations together (Table 2).

To create the matrix of dispersal probabilities between the 11 putative populations, we first traced the pairwise shortest marine geographical distances (Fig. 1b) and set low dispersal rates between populations separated by depths greater than 200 m, as the modelled species is found in shallower waters (Quéro and Vayne 1997). Given the lack of information on potential migrations between the 11 putative populations, two somewhat arbitrary dispersal scenarios were tested. The first scenario corresponded to a strong potential for dispersal and the second to a more sedentary behavior. In the first scenario, the dispersal probability between adjacent populations i and j was set to $d_{ij} = 0.1$ between putative populations WC and Ir and BC and EC (see Fig. 1b) and to 0.2 for the other adjacent populations. Dispersal probabilities between more distant populations were obtained by accounting for the number of populations between the origin and arrival population along the dispersal tracks in Fig. 1b, e.g., dispersal between WB and CS populations via BoB was set to $0.2 \times 0.2 = 0.04$. The probability to remain in the same population was calculated as $d_{ii} = 1 - \sum_{j=1}^{10} d_{ij}$; it decreased with increasing number of direct neighbours. Note that in this scenario dispersal probabilities were symmetrical, i.e., $d_{ij} = d_{ji}$. The full dispersal matrix can be found in Supplementary Table S2[1].

In the second dispersal scenario, the probability d_{ii} to remain in the same population was fixed between 0.75 and 0.99 according to the size of the neighbourhood, with smaller values for geographically more central populations. Dispersal probabilities d_{ij} were a linear function of distance between populations, rescaled so that the sum of all probabilities summed to 1 (Supplementary Table S3[1]). This implied nonsymmetrical dispersal probabilities, i.e., $d_{ij} \neq d_{ji}$. The two dispersal matrices were used for studying demographic and genetic connectivity (Figs. 2a, 2b).

For genetic connectivity estimation (see below), dispersal was assumed to occur before the first birthday of egg laying only. This

Fig. 2. Dispersal probabilities applied for dispersal scenarios 1 (*a*) and 2 (*b*) and population abundances assumed for genetic and demographic connectivity studies (*c*). For population abbreviations, see Fig. 1b.
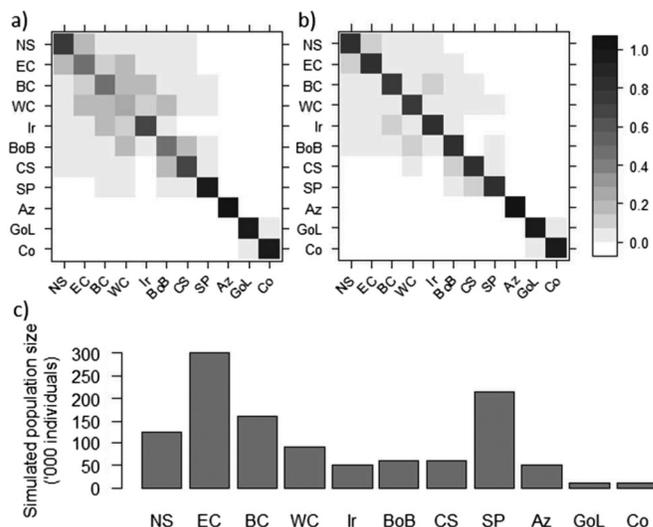
is equivalent to assuming that each individual reproduces in one population only during its life, either in its native population or in the one it dispersed to. This type of behavior has been observed for several fish species, with individuals breeding several years in the same area (Dittman and Quinn 1996; Feldheim et al. 2014; Bonanomi et al. 2016). For example, Bonanomi et al. (2016) found that Atlantic cod (*Gadus morhua*) can disperse more than 1000 km from their place of birth and spend several years growing in the place they dispersed to before returning as mature individuals to their place of birth for breeding. Natal philopatry is well-described for sharks (Feldheim et al. 2014) but not for skates and rays. However, for the thornback ray, a study using data storage tags indicated that most individuals were philopatric with a maximum travelling distance of 130 km (Hunter et al. 2005a, 2005b).

Population abundance

To derive population abundances for the 11 putative populations, recent international landings were used (ICES 2016; FAO 2016). The Eastern (English) Channel (EC) population had the highest landings and the Gulf of Lion population the lowest (Table 2; Fig. 1a). As little regional information was available, landings in biomass were considered reflecting relative population abundances in numbers. For computational reasons, the maximum population abundance, corresponding to the population in the EC, was fixed to 300 000 individuals; this is of course much smaller than the actual population size. The abundance of the other populations, except for the two Mediterranean populations, was then set applying the ratio between their landings and those of the EC. For the two Mediterranean populations, instead of the corresponding number of individuals, 10 000 individuals were assumed to avoid too small numbers (Table 2; Fig. 2c). These population abundances will be referred to as N_0 below.

Genetic connectivity

Among the many simulators available for population genetics studies, only a few are designed to account for complex life histories and large population abundances. The R package MetaPopGen (v3.1.2; R Development Core Team 2008; v0.0.4; Andrello and Manel 2015) is such a simulator; it can simulate population genetic data for species with complex life history traits (overlapping generations, age-specific survival and fecundity, etc.) in a reasonable time but can simulate only one locus.

The simulations were set up to follow as much as possible the life cycle of medium-sized rays and skates taking the thornback ray as model. Yearly, each mature individual produced gametes according to its fecundity and sex. Fecundity was fixed to 140 gametes for females and 10 000 for males to represent the situation where female gametes are limiting reproduction. Gametes were subject to mutation, with a mutation rate of 1E-06, and fused into eggs with a particular sex and genotype. The dispersed newborns became part of a new population following a recruitment function, which was adapted to correspond to mortality from hatching to age 1. Survival-at-age was as in Supplementary Fig. S1[1].

For both dispersal scenarios, the 11 putative populations were simulated for 10 000 years, repeating the simulations 200 times. This time horizon was selected to study long-term effects of genetic differentiation since the last glacial maximum (Hewitt 2000). Population abundances remained constant at N_0 throughout the whole simulation period (Table 2). Dispersal probabilities varied between populations but were constant during the 10 000 years, as no information on changes in dispersal was available.

For each replicate, one neutral biallelic locus was simulated with an allelic frequency of 0.5 for all populations at the beginning of the simulation (year 0). As our aim was to identify management units based on genetic measures calculated for the whole population (observation errors were ignored) in a simulation framework, one locus was sufficient. Note that the 200 replicates cannot be considered as 200 independent loci, as each replicate had a different number of individuals in year t due to the stochasticity of population and genetic inheritance dynamics. The 11 putative populations were initially undifferentiated in all replicates.

Global and pairwise genetic differentiation between putative populations was estimated using the fixation index F_{ST} (Hamilton 2009) for each replicate and simulation year:

$$(6) \qquad F_{ST} = (H_T - H_S)/H_T$$

where H_T is the heterozygosity in the pooled putative populations, and H_S is the mean heterozygosity in each population. Mean and median global F_{ST} were calculated over the 200 replicates.

To evaluate the contribution of the difference in abundance to genetic differentiation, we also simulated 11 putative populations with identical population abundances (10 000 individuals). From this simulation we selected population pairs leading to $F_{ST} > 0.001$; $F_{ST} < 0.001$ were considered to indicate absence of genetic differentiation, in which case differences in abundance cannot play a role. This threshold value was obtained from the relationship between pairwise F_{ST} values and the mean number of migrants between pairs (see Results).

The effect of differences in abundance on F_{ST} values was evaluated by calculating the ratio between the F_{ST} values of the selected pairs ($F_{ST} > 0.001$) for simulations with identical abundance and for simulations with different abundances as described above. These ratios of F_{ST} values were then linearly regressed on the absolute difference in abundance between pairs of exchanging populations.

Demographic connectivity

For studying global demographic connectivity C for each putative population i, the relative change in abundance after a single dispersal event was calculated as

$$(7) \qquad C_i = \frac{-N_{0i}\sum_{j \neq i} d_{ij} + \sum_{j \neq i} d_{ji} N_{0j}}{N_{1i}}$$

where N_{0i} is the abundance before the dispersal event for population i (see Table 2), N_{1i} is the abundance after the dispersal event for population i, and d_{ij} is the dispersal rate from population i to population j as described above. This approach was chosen as life history parameters were not available for all putative populations, making it impossible to use a more detailed dynamic modelling approach. Further, considering a short-term perspective is in line with the requirement that exchanges between connected populations have to occur in most years for using them as basis for defining management units (Hawkins et al. 2016).

The origin of individuals in each population i after a single dispersal event was then investigated by calculating the proportion of individuals in population i that came from population j, $P_{i|j}$, as follows:

$$(8) \qquad P_{i|j} = \frac{N_{0j} d_{ji}}{N_{1i}}$$

This metric $P_{i|j}$ is referred to as pairwise demographic connectivity.

Waples and Gaggiotti (2006) and Palsbøll et al. (2007), based on Hastings (1993), considered that populations linked by ≥10% migrants should be assigned to the same management unit. We therefore compared pairwise demographic connectivity estimates $P_{i|j}$ with the threshold value of 0.1. This choice is somewhat arbitrary and will be discussed below.

To evaluate the contribution of the difference in abundance to demographic connectivity, we also calculated the pairwise demographic connectivity between the 11 putative populations with identical population abundances (10 000 individuals). Then, we selected population pairs leading to $P_{i|j} > 0.1$. As for genetic connectivity, the effect of differences in abundance on the demographic connectivity values was evaluated by calculating the ratio between the $P_{i|j}$ values of the selected pairs with identical abundance and the $P_{i|j}$ values of the same pairs with different abundance. These ratios of $P_{i|j}$ values were then linearly regressed on the difference in abundance between pairs of exchanging populations.

Fig. 3. (*a*) Local parameter elasticity and (*b*) global Morris sensitivity analysis results for the Usher matrix model for thornback ray. For parameter definitions and values, see Table 1.

Fig. 4. Density of simulated global genetic differentiation F_{ST} for 200 replicate trajectories for dispersal scenarios 1 (*a*) and 2 (*b*). Black solid line: median; black dotted line: mean; grey solid line: maximum. Index of pairwise genetic differentiation F_{ST} between all pairs of populations at the end of the simulations (10 000 years) averaged for 200 replicates for dispersal scenarios 1 (*c*) and 2 (*d*). For population abbreviations, see Fig. 1*b*.

Results

Life history parameters and intrinsic population growth

Using the reference parameter values in the Usher matrix model, at equilibrium, 41% of individuals were 1 year old (stage 1), 39% immature (stage 2), and 20% mature (stages 3 and 4), among which 13% belonged to the stage 4 category representing mature individuals with a larger number of eggs.

Local elasticity analysis identified the survival of stage 3 individuals (S_3) as the parameter to which intrinsic population growth was the most reactive, while it was least reactive (and reacting negatively) to the rate of fecundity increase from stage 3 to stage 4 (H_3) (Fig. 3*a*); similar results were obtained for the set of alternative parameter values and when varying parameter values by ±10%. All elasticity values were <0.2 except for S_3 and S_2, thus indicating a degree of robustness to parameter value changes.

Results of the global sensitivity analysis (Morris method) differed from the local elasticity analysis (Fig. 3*b*). S_0 was the parameter with the highest influence on intrinsic population growth (λ) changes and the highest strength of interactions (large σ^2), directly followed by S_1, S_2, and H_2. Changes in parameters S_3, S_4, and H_3 had little influence on λ. These parameters interacted little, with the smallest value for σ^2 reached by H_3. The influence of the number of eggs Ω_4 was intermediate.

From these complementary analyses, it appeared that survival rates of immature individuals (S_0, S_1, and S_2) were the parameters to which the population growth rate was most sensitive. On the other hand, parameters linked to the mature stages (S_3, S_4, and H_3) appeared less important in terms of contribution to changes in λ and interactions with others parameters.

Genetic connectivity

Two hundred replicates were sufficient to capture stochastic variations (not shown). The median final global differentiation index (F_{ST}) between the 11 putative populations after 10 000 years of divergence was low, 0.014 (95% confidence interval (CI): 0.0010–0.044) and 0.013 (95% CI: 0.0012–0.042) for dispersal scenario 1 (strong dispersal) and scenario 2 (strong sedentary behavior), respectively (solid lines, Figs. 4*a* and 4*b*). For both scenarios, simulated F_{ST} trajectories varied strongly among replicates leading to a standard deviation between replicates of 0.12 in the final year. Note that even after 10 000 years of simulation, no equilibrium was reached.

Plotting mean pairwise F_{ST} values after 10 000 years against the mean number of migrants revealed that F_{ST} values were >0.001 for small number of migrants (<5 individuals) between population pairs (Fig. 5*a*). The threshold value 0.001 was therefore used for identifying genetically disconnected populations. Note that small pairwise F_{ST} values occurred even though there were very few pairwise migrants (pairs in bottom left corner of Fig. 5*a* with

Fig. 5. (*a*) Mean pairwise F_{ST} of simulations plotted against the mean number of annual migrants from population *i* to population *j* and vice versa and (*b*) ratio between pairwise F_{ST} of simulations with identical abundance for all populations and pairwise F_{ST} > 0.001 of simulations with different abundances as a function of the pairwise difference of these abundances. In panel (*a*), the continuous horizontal line indicates the threshold value of 0.001 used in this study. Note that the *x* axis in panel (*a*) was cut at 30 migrants; all F_{ST} values beyond this value are below the threshold value. All population pairs have a single simulated F_{ST} value but two sets of number of migrants (one in each direction), which are linked by lines. SC; dispersal scenario.
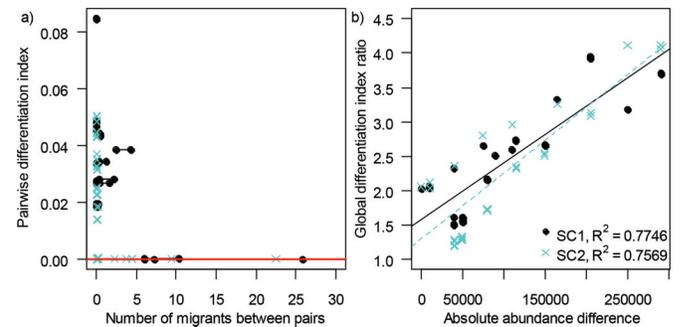
<1 migrant). This is due to the existence of multiple connections for certain populations.

For both dispersal scenarios, analysis of pairwise genetic differentiation between putative populations revealed high genetic differentiation between the Azores (Az) and the other populations (F_{ST} > 0.03 after 10 000 years; Figs. 4*c* and 4*d*). Mediterranean populations (GoL and Co) were also differentiated from the other

populations (mean $F_{ST} > 0.035$). This was not surprising given the assumed geographic isolation of both the Az and Mediterranean populations. Mediterranean populations were more differentiated ($F_{ST} \approx 0.1$) from the Az population than from Atlantic populations mainly due to lower assumed dispersal rates but also due to smaller population sizes (Figs. 4c and 4d). The simulations with identical populations sizes (10 000 individuals) confirmed that in this case genetic differentiation patterns were driven by the assumed dispersal patterns, with Mediterranean populations being again more differentiated from Az compared with the Atlantic populations (not shown).

For dispersal scenario 1, after 10 000 years, Atlantic populations (except Az) were not genetically differentiated from each other, i.e., pairwise F_{ST} values were ≪0.001 (Fig. 4c; Table 2). Only South Portugal (SP) presented a weak genetic differentiation from more northern populations ($F_{ST} = 0.0005$ compared with 0.00002 between the northern populations). The two Mediterranean populations formed two units with low genetic heterogeneity ($F_{ST} = 0.002$).

For dispersal scenario 2, Atlantic populations (except Az) were more structured (globally higher F_{ST} value than for scenario 1) but not genetically differentiated from each other applying the threshold value of 0.001 (Fig. 4d; Table 2). Using a lower threshold of $F_{ST} > 0.0001$ for determining populations, Atlantic populations appeared more structured with two groups (Supplementary Table S5[1]). In this case the northern group was composed of the North Sea (NS), the EC, the Bristol Channel (BC), and the Ireland (Ir) populations. The southern group was composed of the Cantabrian Sea (CS) and SP. Finally, the Bay of Biscay (BoB) population was differentiated with all other populations except the Western Channel (WC) population.

The two patterns of genetic differentiation between the 11 putative populations primarily but not exclusively reflected dispersal patterns, as relative differences in population sizes also played a role. For example, in scenario 1, differentiation between Az and EC was weaker than differentiation between Az and BoB despite an identical dispersal rate. To visualize this abundance effect, the ratio of F_{ST} values obtained assuming identical population abundances and population-specific abundances (N_0) was regressed against the absolute value of the difference in population-specific abundances. For both dispersal scenarios, this relationship was linear and rather similar (Fig. 5b). Thus, the difference found in the pairwise F_{ST} of the Az population with EC compared with BoB was due to the difference in abundance (Figs. 4c and 4d).

Demographic connectivity

The two dispersal scenarios led to qualitatively similar results in terms of global demographic connectivity, i.e., annual net contributions of dispersing individuals to the different putative populations (Figs. 6b and 6d and Supplementary Tables S6 and S7[1]). The biggest source population was the EC, which had an annual net loss of −15% and −4% for dispersal scenario 1 (strong dispersal) and scenario 2 (strong sedentary behavior), respectively. The annual net losses for the BC population were −7% and −2% for dispersal scenarios 1 and 2, respectively. For SP, these were −1% and −4%, respectively. Az, East Corsica (Co), and Gulf of Lion (GoL) populations had minor exchanges with the other populations, while all other populations experienced net gains for both dispersal scenarios. More precisely, the populations near Ir and in WC (including Southern Celtic Sea) gained most under dispersal scenario 1 (+18% and +16%), while for dispersal scenario 2 the biggest net gain was found for the CS population (+12%), followed by the Ir population (+10%).

Considering only population pairs linked by pairwise demographic connectivity of more than the 10% threshold value, 13 pairs of demographically closely linked populations emerged for dispersal scenario 1 (Fig. 6a). Three pairs exchanged reciprocally more than 10% of individuals: (i) the EC and the NS, (ii) the EC and the BC, and (iii) the BoB with the CS. For the two first pairs, if we

Fig. 6. Pairwise percentage of individuals exchanged by putative population i (rows) with population j (columns), i.e., pairwise demographic connectivity for dispersal scenarios 1 (a) and 2 (c). Overall net percentage of individuals lost (negative value) or gained (positive value) by each putative population are also shown for dispersal scenarios 1 (b) and 2 (d). For geographic location of populations, see Fig. 1b. (e) Ratio between pairwise demographic connectivity of population with identical abundance and pairwise demographic connectivity of population with different abundances as a function of the pairwise difference of these abundances. SC: dispersal scenario.
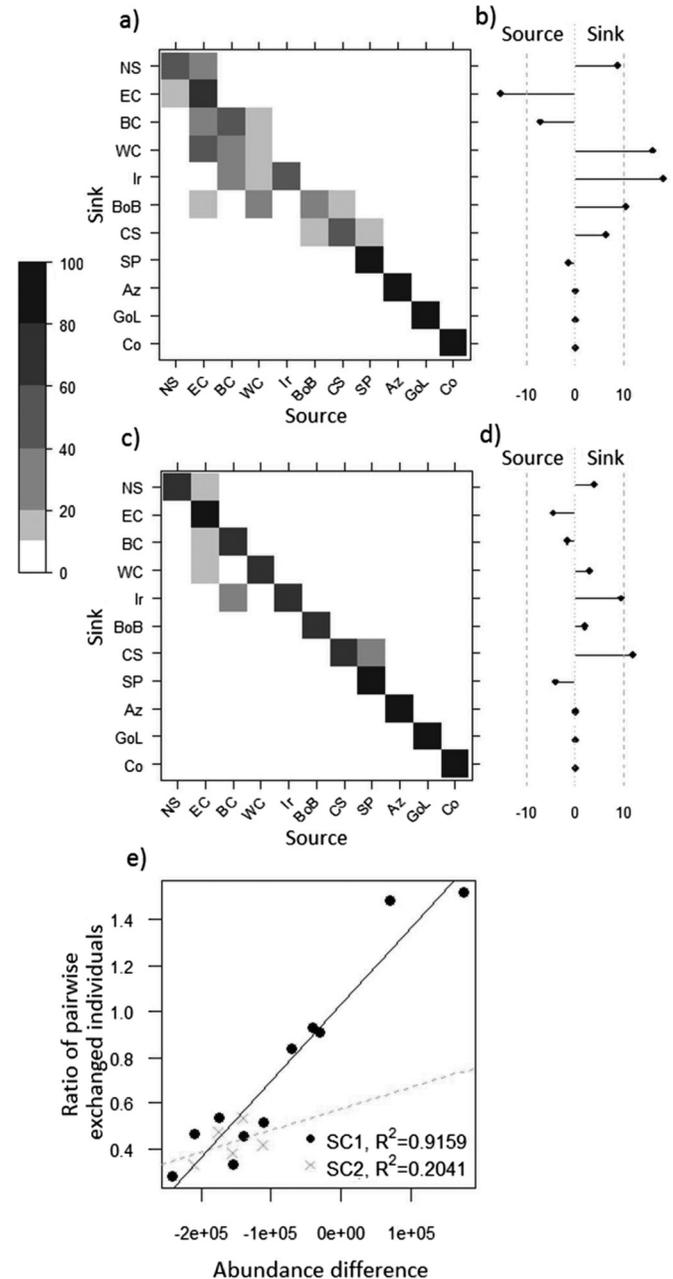
look at net exchanges, the EC appeared to be a source while the NS and the BC were sinks. For the seven other pairs, only one of the two received more than 10% of individuals from the other (Fig. 6a): BC and EC, WC and EC, Ir and BC, Ir and WC, BoB and EC, BoB and WC, and CS and SP (the first populations is the sink and the second the source). In summary, for scenario 1 the English Channel was

the main source of individuals for the other putative Northeast Atlantic populations.

For dispersal scenario 2, only five pairs of demographically closely linked populations (>10%) emerged (Fig. 6b): NS and EC, BC and EC, WC and EC, Ir and BC, and SC and SP (the first population is the sink and the second the source). None of the links were reciprocal. Overall in this scenario, populations appeared to be less connected, and the main sources appeared to be SP and again EC, which were also populations with the highest assumed abundances.

Based on these results, a number of groups of linked populations emerged where each group could be considered to represent a single metapopulation (Table 2). For dispersal scenario 1, four metapopulations could be identified: the first one comprising the Northeast Atlantic populations from the NS to the SP, the second one being constituted by the Az, and the last two by the two Mediterranean populations (GoL and Co). Focusing only on reciprocal links (>10% for both receiving and donor population), the four previous metapopulations subdivided into eight: NS together with EC; BC together with WC, Ir, and BoB; CS together with S, Az, and GoL; and finally Co. In contrast, for scenario 2, six metapopulations emerged (Fig. 6c). The first one grouping populations from the NS to Ir, the second one including only BoB, the third one grouping CS and SP, while the fourth to the sixth metapopulations were similar to those found for scenario 1 (Az, GoL, Co). Again considering only pairs with reciprocal links, all 11 putative populations were demographically independent and hence should be managed separately under this dispersal scenario.

Abundance differences also played a role for demographic connectivity (Fig. 6e). To visualize this abundance effect, the ratio of $P_{i|j}$ values obtained assuming identical population abundances, and population-specific abundances (N_0) were regressed against the difference in population-specific abundances (not absolute difference as for genetic connectivity; Fig. 6e). For both dispersal scenarios, this relationship was linear and positive, though rather weak for scenario 2 in contrast with genetic connectivity for which no difference between scenarios was found (Fig. 5b).

Discussion

Population growth

Analyzing the elasticity and sensitivity of the intrinsic population growth rate in the Usher matrix model for a thornback ray-like species, we found that it was most sensitive to survival from egg laying to stage 1 (S_0), followed by the survival of stages 1 and 2 (S_1 and S_2), and least sensitive to the maturation rate (H_3), that is to the proportion of mature individuals moving to stage 4 with higher fecundity. This result likely applies to other ray and skate species that share the late age-at-maturity, and hence probably similar survival rates, and low fecundity as for thornback ray (Supplementary Table S1[1]).

Given survival during the early stages is such an important parameter for population dynamics, it would be important to obtain field estimates for each population. Unfortunately, we do not know of any in situ method for estimating first year survival. For older individuals, capture–mark–recapture methods might be feasible (e.g., Neat et al. 2015).

Population connectivity

Genetic simulation results indicated a strong influence of assumed dispersal rates on genetic population structure, though population abundance differences were found to substantially modify the effect of contrasting dispersal rates (Fig. 5). This result is not surprising, as the level of genetic differentiation among populations is directly related to the balance between gene flow (related to dispersal) and genetic drift (somewhat related to population abundance) (Wright 1949; Palumbi 2003; Waples and Gaggiotti 2006). Genetic connectivity simulations indicated four

metapopulations (Table 2): the first along the Atlantic continental shelf, the second around the Azores (whose structure was not studied here), and the third and fourth in the Gulf of Lion and around Corsica, which globally agrees with the empirical genetic result found by Chevolot et al. (2006). However, it is important to remember that genetic connectivity studies provide information on an evolutionary time scale. A low genetic differentiation does not necessarily imply a contemporary high number of migrants because the time needed for genetic differentiation depends upon the number of breeders in each population. In large populations with low genetic drift, very low migration rates would maintain genetic similarity between populations that became physically separated (Reiss et al 2009).

Genetic connectivity has been studied for several ray and skate species, highlighting substantial differentiations among the studied locations (Chevolot et al. 2006; Frodella et al. 2016; Vargas-Caro et al. 2017). For example, Pasolini et al. (2011) found a genetic population structure in the eastern Atlantic for thornback ray and biscuit skate (*Raja straeleni*) and a significant correlation between genetic differentiation and coastal distance. However, for several species, including thornback ray, a major limitation to dispersal appeared to be bathymetry (Chevolot et al. 2006; Pasolini et al. 2011; Le Port and Lavery 2012).

Pairwise demographic connectivity indicated four (dispersal scenario 1) or six (dispersal scenario 2) metapopulations compared with only four for genetic connectivity (Table 2). Demographic-based metapopulations were defined as groups of putative populations for which, for sink populations, a single dispersal event resulted in at least 10% of individuals coming from another of the subpopulations (source population) within the metapopulation. The 10% threshold value is rather arbitrary. It was inspired by the value used for judging the importance of dispersal rates (Waples and Gaggiotti 2006; Palsbøll et al. 2007). Doubling the threshold value to 20% would increase the number of demographic metapopulations to six (scenario 1) and nine (scenario 2), respectively.

A strong effect of the difference in population abundances on genetic and demographic connectivity was found for dispersal scenario 1, but only for genetic connectivity for scenario 2. In scenario 2, most individuals stayed at their population of origin, which meant differences in population abundance played less a role for a single dispersal event considered for demographic connectivity.

The ICES currently considers six thornback ray stocks in the Northeast Atlantic, based upon ICES ecoregions, discontinuities in the species geographical distribution, and expert knowledge (Table 2). The connectivity-based metapopulation results disagreed with the current stock assessment units in several ways: the Bay of Biscay and Cantabrian Sea ICES stock was subdivided based on demographic results for dispersal scenario 2, while the Bristol Channel and Northern Celtic Sea stock as well as the Western Channel and Southern Celtic Sea stock were grouped with the Eastern Channel and the North Sea stocks based on genetic and demographic connectivity (both dispersal scenarios; Table 2). However, field studies are needed to confirm the identified metapopulation structure before any recommendations for changing stock assessment units can be made. As current management units for skates and rays are not aligned to stock assessment units, a complete revision of the management of skate and ray fisheries in European waters would be needed in a second step.

The results concerning potential metapopulation structures differed somewhat between demographic and genetic connectivity, with more populations being genetically connected than demographically. This phenomenon was empirically observed in shark and named crinkled connectivity (Ovenden 2013). It occurs when migration is above the threshold required to link populations genetically, but below the threshold for demographic links (Ovenden 2013). This difference between genetic and demographic connectivity is not surprising, as they provide informa-

tion on different temporal and geographical scales. Demographic data help define management units, provided that a specific threshold value for the exchange of individuals can be defined. Genetic studies provide large-scale differentiation information integrated over a longer time period, making results at a local scale and for shorter time periods less pertinent for management.

Connectivity is driven by the dispersal of individuals. Traditional stock assessment and fisheries management generally consider stocks as closed populations. However, if exploited stocks are not closed populations, the contributions of dispersals need to be considered in management (Frisk et al. 2014). This can be especially important for skates and rays where only juveniles and adults move. For example, winter skate (*Leucoraja ocellata*) abundance increased strongly on Georges Bank in the 1980s, which appeared biologically unrealistic. Frisk et al. (2008) suggested that this increase was due to movements among adjacent populations, thus connectivity.

Dispersal increases the number of individuals of the receiving population and thus is equivalent to an increase in survival. Assuming dispersal occurs only during the first year of life, we can express the calculated net contributions of immigrants to the 11 putative populations in terms of a change in first year survival rate. Assuming $S_0 = 0.036$ (baseline value in Table 1), an increase of 18% (maximum estimated net gain due to demographic connectivity) is equivalent to increasing the survival rate to $S_0 = 0.042$, while a 15% decrease (maximum estimated net loss) corresponds to $S_0 = 0.031$. This range of first year survival rates is small compared with the uncertainty surrounding realistic values. An increased survival rate of $S_0 = 0.042$ lead to an increase of the intrinsic growth rate of 2.26%, and a decreased survival rate of $S_0 = 0.031$ lead to a decrease of the intrinsic growth rate of 2.11%.

Methodology

Several assumptions were needed to overcome the lack of data and biological knowledge. In the Usher model, first year survival (S_0) was set conditional on other parameter values and assuming a stable population. The resulting survival rate might appear high compared with teleost species (0.036 in Table 1). This parameter combines the mortality of eggs and newly hatched individuals. Skates and rays do not provide any parental care, making the rigid keratin capsule the only protection against predators (Kormanik 1993), and so egg mortality is primarily caused by predation (Bunn et al. 2000; Cox et Koob 1993). Lucifora and Garcia (2004) reported gastropod predation rates around 0.24 for four ray species in the Southwest Atlantic. The sensitivity and elasticity analyses showed that this parameter was influential for the population dynamics of a thornback ray-like species; a similar importance can be assumed for other skates and rays in European waters, which share similar life history traits (Supplementary Table S1[1]).

Several assumptions were also necessary to study population connectivity. Absolute abundance estimates currently do not exist for any of the ray and skate populations in European waters (ICES 2016). Relative population abundances were derived by assuming that commercial landings represented relative population abundances. In quota-based fisheries management systems, landings do not directly inform on population abundance. However, under the current management in Europe, the quota is set for a pool of several rays and skates and there is no regulatory minimum landing size at species level, and this in turn makes quotas less restrictive at species-specific level. Thus, in this case, commercial landings might approximately reflect relative population biomass and abundance if mean mass is similar across populations. Changing the relative abundances of the 11 putative populations would modify estimated demographic and genetic connectivity patterns and absolute values; the degree of this would depend on by how much proportions were changed.

Population abundances were assumed fixed but are known to vary over time. For example, bottom trawl surveys have shown abundance variations in recent years, including a dramatic increase of thornback ray in the Eastern Channel over the last decade (ICES 2016). In contrast, a recent study of thornback ray population dynamics in the Bay of Biscay suggested no increase in recent years (Marandel et al. 2016). At an evolutionary time scale, over the 10 000 years simulated for genetic connectivity, sea level and temperature increases probably triggered changes in population distributions and abundances. Thus, the constant dispersal rates and population abundances that we used should not be taken as realistic either in genetic or demographic terms. The results should rather be regarded as indicative of the potential magnitude of the contrast between the genetic and demographic connectivity. However, if times series of abundance estimates were available for all putative populations, these might be used directly for studying demographic connectivity by analysing synchronism in interannual abundance variations (Östman et al. 2017).

In genetic simulations due to computational limits, simulated population abundances were much smaller than likely actual abundances. However, this did not affect the spatial pattern of genetic differentiation, only the absolute F_{ST} values, which might be higher in our simulations than in actual populations, as in reality their larger number is expected to reduce genetic drift.

In the absence of dispersal rate estimates for all putative populations, two scenarios, expected to reflect a plausible range of dispersal for the species, were investigated. The first one corresponded to a strong potential for dispersal and the second one to a stronger sedentary behavior. Simulating more extreme scenarios would basically reflect that with high dispersal rate panmixia is maintained, and with low dispersal rate, all populations differentiate. To carry out more realistic simulations, it would be necessary to estimate dispersal of all populations in the field. Several methods are available for this. Telemetry can provide estimates of individual movements between populations and of behavior patterns (Milner-Gulland and Rowcliffe 2007; Hawkins et al. 2016). For conventional tagging, due to often low reported recapture rate (6.9%; Stephan et al. 2015), a high number of individuals has to be tagged and released to be able to estimate dispersal rate with reasonable uncertainty. Electronic data storage tags allows for obtaining information from a higher proportion of tagged individuals (Hunter et al. 2006); however, cost may be prohibitive. This method was used for tracking basking sharks (*Cetorhinus maximus*; Sims et al. 2003, 2005) and studying thornback rays stock distribution in the southern North Sea (Hunter et al. 2006).

For genetic connectivity, dispersal was assumed to occur for newborns only. This is equivalent to assuming that each individual reproduces in one population only during its life, either in its native population or in the one it dispersed to before maturing. Thus, the assumed dispersal rates should be considered as the contribution of dispersal to each population and not as the individual contribution. If the assumed dispersal rates were applied to all ages, genetic connectivity could be modified, as the age of the disperser will affect the number of years during which it will reproduce in the receiving population and so will differently affect the gene pool.

Genetic connectivity was modelled by simulating a neutral marker. Neutral loci have been recommended for identifying management units (Funk et al. 2012). However, in the case of recently differentiated populations with large population size, markers under selection may be more efficient (Reiss et al. 2009; Gagnaire et al. 2015). Using non-neutral markers in simulations would require assumptions on the dynamics of selection. Local adaption might mean that immigrants have lower fitness, which would reduce their contribution to genetic connectivity, as their genotypes would be less integrated into the local gene pool. As a consequence, their contribution to population dynamics could be

modified and demographic connectivity reduced. Therefore, if adaptation to regional environment has occurred, both genetic and demographic connectivity could be lower than estimated in this study.

Demographic connectivity was studied applying a single dispersal event to the assumed population abundances. Given these abundances were derived from recent landings, their relative proportions might be expected to reflect the contemporary situation, in which case applying a single dispersal event would be informative for current management. Contrary to species for which dispersal primarily occurs during the larval phase and for which ocean current models can be used to predict connectivity, there is no reason to believe that thornback ray, or any other ray or skate for that matter, would follow bottom currents. Thus, to develop a more complex dynamic model, knowledge on factors determining individual dispersal, survival, and reproduction would be needed for all putative populations. None of these are currently available.

Conclusion

Demographic and genetic connectivity can provide complementary insights for medium-sized rays and skates as we demonstrated with the example of thornback ray. Genetic connectivity studies should be useful for determining long-term conservation units but will probably not be so helpful for defining management units, while demographic connectivity studies should be able to inform the definition of management units. Both types of analyses strongly depend on relative population abundances (Figs. 5 and 6e) but also on dispersal rates and patterns. To make progress towards a better estimation of connectivity and delimitation of management and conservation units, we encourage researchers to attempt obtaining local abundance and dispersal estimates for a range of ray and skate species.

Acknowledgements

References

Andrello, M., and Manel, S. 2015. MetaPopGen: an r package to simulate population genetics in large size metapopulations. Mol. Ecol. Resour. **15**(5): 1153–1162. doi:10.1111/1755-0998.12371.

Bonanomi, S., Overgaard Therkildsen, N., Retzel, A., Berg Hedeholm, R., Pedersen, M.W., Meldrup, D., Pampoulie, C., Hemmer-Hansen, J., Grønkjaer, P., and Nielsen, E.E. 2016. Historical DNA documents long-distance natal homing in marine fish. Mol. Ecol. **25**(12): 2727–2734. doi:10.1111/mec.13580. PMID:26859133.

Bunn, N.A., Fox, C.J., and Webb, T. 2000. A literature review of studies on fish egg mortality: implications for the estimation of spawning stock biomass by the annual egg production method. Technical Report, Cefas Science Series.

Campolongo, F., Cariboni, J., and Saltelli, A. 2007. An effective screening design for sensitivity analysis of large models. Environ. Model. Softw. **22**(10): 1509–1518. doi:10.1016/j.envsoft.2006.10.004.

Caswell, H. 2001. Matrix population models: construction, analysis, and interpretation. 2nd ed. Sinauer Associates, Sunderland, Mass.

Chevolot, M. 2006. Assessing genetic structure of thornback ray, *Raja clavata*: a thorny situation? Thesis, University of Groningen.

Chevolot, M., Hoarau, G., Rijnsdorp, A.D., Stam, W.T., and Olsen, J.L. 2006. Phylogeography and population structure of thornback rays (*Raja clavata* L., Rajidae). Mol. Ecol. **15**(12): 3693–3705. doi:10.1111/j.1365-294X.2006.03043.x. PMID:17032267.

Chevolot, M., Wolfs, P.H.J., Pálsson, J., Rijnsdorp, A.D., Stam, W.T., and Olsen, J.L. 2007. Population structure and historical demography of the thorny skate (*Amblyraja radiata*, Rajidae) in the North Atlantic. Mar. Biol. **151**(4): 1275–1286. doi:10.1007/s00227-006-0556-1.

Cox, D.L., and Koob, T.J. 1993. Predation on elasmobranch eggs. Environ. Biol. Fishes, **38**(1–3): 117–125. doi:10.1007/BF00842908.

Davidson, L.N.K., Krawchuk, M.A., and Dulvy, N.K. 2016. Why have global shark and ray landings declined: improved management or overfishing? Fish Fish. **17**(2): 438–458. doi:10.1111/faf.12119.

Delpiani, G. 2016. Reproductive biology of the southern thorny skate *Amblyraja doellojuradoi* (Chondrichthyes, Rajidae): reproduction of *Amblyraja doellojuradoi*. J. Fish Biol. **88**(4): 1413–1429. doi:10.1111/jfb.12917. PMID:26923668.

Dingle, H. 2014. Migration: the biology of life on the move. 2nd ed. Oxford University Press, Oxford, New York.

Dittman, A., and Quinn, T. 1996. Homing in Pacific Salmon: mechanisms and ecological basis. J. Exp. Biol. **199**: 83–91. PMID:9317381.

Dulvy, N.K., Fowler, S.L., Musick, J.A., Cavanagh, R.D., Kyne, P.M., Harrison, L.R., Carlson, J.K., Davidson, L.N., Fordham, S.V., Francis, M.P., Pollock, C.M., Simpfendorfer, C.A., Burgess, G.H., Carpenter, K.E., Compagno, L.J., Ebert, D.A., Gibson, C., Heupel, M.R., Livingstone, S.R., Sanciangco, J.C., Stevens, J.D., Valenti, S., and White, W.T. 2014. Extinction risk and conservation of the world's sharks and rays. eLife, **3**: e00590. doi:10.7554/eLife.00590. PMID:24448405.

Ellis, J.R., and Shackley, S.E. 1995. Observations on egg-laying in the thornback ray. J. Fish Biol. **46**(5): 903–904. doi:10.1111/j.1095-8649.1995.tb01613.x.

FAO. 2016. Fisheries and Aquaculture Department, Statistics and Information Service. FishStat: Universal software for fishery statistical time series [online]. Available from http://www.fao.org/fishery/statistics/en. FAO, Rome.

Feldheim, K.A., Gruber, S.H., DiBattista, J.D., Babcock, E.A., Kessel, S.T., Hendry, A.P., Pikitch, E.K., Ashley, M.V., and Chapman, D.D. 2014. Two decades of genetic profiling yields first evidence of natal philopatry and long-term fidelity to parturition sites in sharks. Mol. Ecol. **23**(1): 110–117. doi:10.1111/mec.12583. PMID:24192204.

Frisk, M.G., Miller, T.J., Martell, S.J.D., and Sosebee, K. 2008. New hypothesis helps explain elasmobranch "outburst" on Georges Bank in the 1980s. Ecol. Appl. **18**(1): 234–245. doi:10.1890/06-1392.1. PMID:18372569.

Frisk, M.G., Jordana, A., and Miller, T.J. 2014. Moving beyond the current paradigm in marine population connectivity: are adults the missing link? Fish Fish. **15**(2): 242–254. doi:10.1111/faf.12014.

Frodella, N., Cannas, R., Velonà, A., Carbonara, P., Farrell, E., Fiorentino, F., Follesa, M., Garofalo, G., Hemida, F., Mancusi, C., Stagioni, M., Ungaro, N., Serena, F., Tinti, F., and Cariani, A. 2016. Population connectivity and phylogeography of the Mediterranean endemic skate *Raja polystigma* and evidence of its hybridization with the parapatric sibling *R. montagui*. Mar. Ecol. Progr. Ser. **554**: 99–113. doi:10.3354/meps11799.

Funk, W.C., McKay, J.K., Hohenlohe, P.A., and Allendorf, F.W. 2012. Harnessing genomics for delineating conservation units. Trends Ecol. Evol. **27**(9): 489–496. doi:10.1016/j.tree.2012.05.012. PMID:22727017.

Gagnaire, P.-A., Broquet, T., Aurelle, D., Viard, F., Souissi, A., Bonhomme, F., Arnaud-Haond, S., and Bierne, N. 2015. Using neutral, selected, and hitch-hiker loci to assess connectivity of marine populations in the genomic era. Evol. Appl. **8**(8): 769–786. doi:10.1111/eva.12288. PMID:26366195.

Gislason, H., Daan, N., Rice, J.C., and Pope, J.G. 2010. Size, growth, temperature and the natural mortality of marine fish: natural mortality and size. Fish Fish. **11**(2): 149–158. doi:10.1111/j.1467-2979.2009.00350.x.

Hallerman, E.M. (*Editor*). 2003. Population genetics: principles and applications for fisheries scientists. American Fisheries Society, Bethesda, Md.

Hamilton, M.B. 2009. Population genetics. Wiley-Blackwell, Chichester, UK; Hoboken, N.J.

Hastings, A. 1993. Complex interactions between dispersal and dynamics — lessons from coupled logistic equations. Ecology, **74**: 1362–1372. doi:10.2307/1940066.

Hawkins, S.J., Bohn, K., Sims, D.W., Ribeiro, P., Faria, J., Presa, P., Pita, A., Martins, G.M., Neto, A.I., Burrows, M.T., and Genner, M.J. 2016. Fisheries stocks from an ecological perspective: disentangling ecological connectivity from genetic interchange. Fish. Res. **179**: 333–341. doi:10.1016/j.fishres.2016.01.015.

Hewitt, G. 2000. The genetic legacy of the Quaternary ice ages. Nature, **405**: 907–913. doi:10.1038/35016000. PMID:10879524.

Hoening, J.M., and Gruber, S.H. 1990. Life-history patterns in the elasmobranchs: implications for fisheries management. NOAA Technical Report.

Holden, M.J., Rout, D.W., and Humphreys, C.N. 1971. The rate of egg laying by three species of ray. ICES J. Mar. Sci. **33**: 335–339. doi:10.1093/icesjms/33.3.335.

Hunter, E., Buckley, A.A., Stewart, C., and Metcalfe, J.D. 2005a. Migratory behavior of the thornback ray, *Raja clavata*, in the southern North Sea. J. Mar. Biol. Assoc. U.K. **85**(5): 1095. doi:10.1017/S0025315405012142.

Hunter, E., Buckley, A.A., Stewart, C., and Metcalfe, J.D. 2005b. Repeated seasonal migration by a thornback ray in the southern North Sea. J. Mar. Biol. Assoc. U.K. **85**(5): 1199. doi:10.1017/S0025315405012300.

Hunter, E., Berry, F., Buckley, A.A., Stewart, C., and Metcalfe, J.D. 2006. Seasonal migration of thornback rays and implications for closure management: ray migration and closure management. J. Appl. Ecol. **43**(4): 710–720. doi:10.1111/j.1365-2664.2006.01194.x.

ICES. 2016. Report of the Working Group on Elasmobranchs Fishes. ICES, Lisbon, Portugal.

Kormanik, G.A. 1993. Ionic and osmotic environment of developing elasmobranch embryos. Environ. Biol. Fishes, **38**(1–3): 233–240. doi:10.1007/BF00842919.

Le Port, A., and Lavery, S. 2012. Population Structure and Phylogeography of the

Short-Tailed Stingray, *Dasyatis brevicaudata* (Hutton 1875), in the Southern Hemisphere. J. Hered. **103**(2): 174–185. doi:10.1093/jhered/esr131. PMID: 22174443.

Levins, R. 1969. Some demographic and genetic consequences of environmental heterogeneity for biological control. Bull. Entomol. Soc. Am. **71**: 237–240.

Lowe, W.H., and Allendorf, F.W. 2010. What can genetics tell us about population connectivity?: Genetic and demographic connectivity. Mol. Ecol. **19**(15): 3038–3051. doi:10.1111/j.1365-294X.2010.04688.x. PMID:20618697.

Lucifora, L.O., and Garcia, V.B. 2004. Gastropod predation on egg cases of skates (Chondrichthyes, Rajidae) in the southwestern Atlantic: quantification and life history implications. Mar. Biol. **145**(5): 917–922. doi:10.1007/s00227-004-1377-8.

Marandel, F., Lorance, P., and Trenkel, V.M. 2016. A Bayesian state-space model to estimate population biomass with catch and limited survey data: application to the thornback ray (*Raja clavata*) in the Bay of Biscay. Aquat. Living Resour. **29**(2): 209. doi:10.1051/alr/2016020.

Milner-Gulland, E.J., and Rowcliffe, J.M. 2007. Conservation and sustainable use: a handbook of techniques. Oxford University Press, Oxford.

Morris, M.D. 1991. Factorial sampling plans for preliminary computational experiments. Technometrics, **33**(2): 161–174. doi:10.1080/00401706.1991.10484804.

Neat, F., Pinto, C., Burrett, I., Cowie, L., Travis, J., Thorburn, J., Gibb, F., and Wright, P.J. 2015. Site fidelity, survival and conservation options for the threatened flapper skate (*Dipturus cf. intermedia*). Aquat. Conserv. Mar. Freshw. Ecosyst. **25**(1): 6–20. doi:10.1002/aqc.2472.

Östman, Ö., Olsson, J., Dannewitz, J., Palm, S., and Florin, A.B. 2017. Inferring spatial structure from population genetics and spatial synchrony in demography of Baltic Sea fishes: implications for management. Fish Fish. **18**: 324–339. doi:10.1111/faf.12182.

Ovenden, J.R. 2013. Crinkles in connectivity: combining genetics and other types of biological data to estimate movement and interbreeding between populations. Marine Freshw. Res. **64**: 201–207. doi:10.1071/MF12314.

Palsbøll, P., Berube, M., and Allendorf, F. 2007. Identification of management units using population genetic data. Trends Ecol. Evol. **22**(1): 11–16. doi:10.1016/j.tree.2006.09.003. PMID:16982114.

Palumbi, S.R. 2003. Populations genetics, demographic connectivity, and the design of marine reserves. Ecol. Appl. **13**(sp1): 146–158. doi:10.1890/1051-0761(2003)013[0146:PGDCAT]2.0.CO;2.

Pasolini, P., Ragazzini, C., Zaccaro, Z., Cariani, A., Ferrara, G., Gonzalez, E.G., Landi, M., Milano, I., Stagioni, M., Guarniero, I., and Tinti, F. 2011. Quaternary geographical sibling speciation and population structuring in the Eastern Atlantic skates (suborder Rajoidea) *Raja clavata* and *R. straeleni*. Mar. Biol. **158**(10): 2173–2186. doi:10.1007/s00227-011-1722-7.

Pujol, G. 2009. Simplex-based screening designs for estimating metamodels. Reliabil. Eng. Syst. Saf. **94**(7): 1156–1160. doi:10.1016/j.ress.2008.08.002.

Pujol, G., Iooss, B., Janon, A. with contributions from Lemaitre, P., Gilquin, L., Le Gratiet, L., Touati, T., Ramos, B., Fruth, J., and Da Veiga, S. 2014. Sensitivity: sensitivity analysis. R package version 1.10.1 [online]. Available from http://CRAN.R-project.org/package=sensitivity.

Quéro, J.C., and Cendrero, O. 1996. Incidence de la pêche sur la biodiversité ichtyologique marine: le Bassin d'Arcachon et le plateau continental Sud Gascogne. Cybium, **20**(4): 323–356.

Quéro, J.-C., and Vayne, J.-J. (*Editors*). 1997. Les poissons de mer des pêches françaises : identification, inventaire et répartition de 209 espèces. Delachaux et Niestlé, Lausanne.

R Development Core Team. 2008. R: a language and environment for statistical computing [online]. R Foundation for Statistical Computing, Austria, Vienna. Available from http://www.R-project.org.

Reiss, H., Hoarau, G., Dickey-Collas, M., and Wolff, W.J. 2009. Genetic population structure of marine fish: mismatch between biological and fisheries management units. Fish Fish. **10**(4): 361–395. doi:10.1111/j.1467-2979.2008.00324.x.

Schnute, J.T., Boers, N., and Haigh, R. 2017. PBSmapping: mapping fisheries data and spatial analysis tools. R package version 2.70.4 [online]. Available from https://CRAN.R-project.org/package=PBSmapping.

Schwartz, M., Luikart, G., and Waples, R. 2007. Genetic monitoring as a promising tool for conservation and management. Trends Ecol. Evol. **22**(1): 25–33. doi:10.1016/j.tree.2006.08.009. PMID:16962204.

Serra-Pereira, B., Figueiredo, I., Farias, I., Moura, T., and Gordo, L.S. 2008. Description of dermal denticles from the caudal region of *Raja clavata* and their use for the estimation of age and growth. ICES J. Mar. Sci. **65**(9): 1701–1709. doi:10.1093/icesjms/fsn167.

Sims, D., Southall, E., Richardson, A., Reid, P., and Metcalfe, J. 2003. Seasonal movements and behaviour of basking sharks from archival tagging: no evidence of winter hibernation. Mar. Ecol. Progr. Ser. **248**: 187–196. doi:10.3354/meps248187.

Sims, D., Southall, E., Metcalfe, J., and Pawson, M. 2005. Basking shark population assessment. Final project report. Global Wildlife Division. Department for Environment, Food and Rural Affairs, London.

Sinclair, A.R.E., Fryxell, J.M., Caughley, G., and Caughley, G. 2006. Wildlife ecology, conservation, and management. 2nd ed. Blackwell Publishing, Malden, Mass.; Oxford.

Stearns, S.C., and Hoekstra, R.F. 2005. Evolution: an introduction. 2nd ed. Oxford University Press, Oxford [England]; New York.

Stephan, E., Gadenne, H., Meheust, E., and Jung, L. 2015. Projet RECOAM : étude de cinq espèces de raies présentes dans les eaux côtières d'Atlantique et de Manche. Rapport final. Association Pour l'Etude et la Conservation des Sélaciens et Laboratoire BioGeMME, Brest, France.

Steven, G.A. 1933. Rays and skates of Devon and Cornwall. III. The proportions of the sexes in nature and in commercial landings and their significance to the fishery. J. Mar. Biol. Assoc. U.K. **18**: 611–625. doi:10.1017/S0025315400043939.

Usher, M.B. 1966. A matrix approach to the management of renewable resources, with special reference to selection forests. J. Appl. Ecol. **3**: 355–367. doi:10.2307/2401258.

Vargas-Caro, C., Bustamante, C., Bennett, M.B., and Ovenden, J.R. 2017. Towards sustainable fishery management for skates in South America: The genetic population structure of *Zearaja chilensis* and *Dipturus trachyderma* (Chondrichthyes, Rajiformes) in the south-east Pacific Ocean. PLoS ONE, **12**(2): e0172255. doi:10.1371/journal.pone.0172255. PMID:28207832.

Walker, P., Howlett, G., and Millner, R. 1997. Distribution, movement and stock structure of three ray species in the North Sea and eastern English Channel. ICES J. Mar. Sci. **54**(5): 797–808. doi:10.1006/jmsc.1997.0223.

Waples, R.S., and Gaggiotti, O. 2006. What is a population? An empirical evaluation of some genetic methods for identifying the number of gene pools and their degree of connectivity. Mol. Ecol. **15**(6): 1419–1439. doi:10.1111/j.1365-294X.2006.02890.x. PMID:16629801.

Waples, R.S., Punt, A.E., and Cope, J.M. 2008. Integrating genetic data into management of marine resources: how can we do it better? Fish Fish. **9**(4): 423–449. doi:10.1111/j.1467-2979.2008.00303.x.

Wright, S. 1949. The genetical structure of populations. Ann. Eugenics, **15**(1): 323–354. doi:10.1111/j.1469-1809.1949.tb02451.x.